https://doi.org/10.15255/KUI.2023.058
KUI-22/2024
Original scientific paper
Received November 22, 2023
Accepted January 19, 2024

Voltammetric Detection of Diclofenac with Screen-printed Electrodes Based on Graphene and PVDF-Modified Graphene

P. Paunović,* *A. Grozdanov*, *I. Dimitrievska*, and *A. Tomova*

Faculty of Technology and Metallurgy, Ss. Cyril and Methodius University in Skopje, Rudjer Bošković 16, Skopje 1000, R. N. Macedonia

Abstract

In recent years, the detection and determination of numerous drugs and pharmaceuticals in various media have become crucial aspects of modern healthcare and environmental management. Among the available sensing techniques, electrochemical methods, particularly those utilising screen-printed electrodes (SPEs) and different portable equipment have emerged as rapid, effective, sensitive, and inexpensive. This study focuses on the detection of the anti-inflammatory drug diclofenac in neutral media. Cyclic voltammetry measurements were conducted to identify diclofenac and determine the kinetics and electrochemical mechanism of its oxidation, along with assessing the surface characteristics of the employed SPEs. Graphene and modified graphene SPEs were explored as nanosensors for this purpose. The surface of the graphene SPE was modified using polyvinylidene fluoride, applied through a drop modification procedure. The morphology of the examined SPEs was observed by means of scanning electron microscope, while the electrolyte (0.1 g of diclofenac per litre of phosphate-buffered solution, pH = 7.4) was analysed using UV-Vis spectroscopy. The results indicate that the studied SPEs exhibit promising potential for the detection of diclofenac.

Keywords

Screen-printed electrodes, nanosensors, cyclic voltammetry, graphene, PVDF drop modification, diclofenac

1 Introduction

One of the most critical priorities in modern healthcare is the detection of pharmaceuticals in various media. This includes identifying active drug compounds in physiological fluids (e.g., plasma), detecting drug residues and growth factors in animal products (milk, meat) and surface water, and ensuring correct drug content while guarding against counterfeit or industrial production error.[1]

Various analytical techniques exist for the detection and quantification of pharmaceutical compounds, encompassing spectroscopic methods (UV-Vis, FTIR, NMR, MASS), chromatographic techniques (HPLC, GC, TLC, HPTLC, UPLC), and electrochemical techniques (voltammetric, potentiometric, amperometric, conductometric)[2,3]. Chromatographic techniques involve a number of pre-preparative steps and elevated costs of laboratory equipment. Compared to the other analytical techniques, electrochemical methods offer several advantages as their application in the analysis of drugs and pharmaceuticals has increased significantly over the last decade.[4,5] Notably, portable potentiostats equipped with screen-printed electrodes (SPEs) have become prevalent in the market, and are recognised for their effectiveness in biological, environmental, medical, and forensic analyses.[6–8]

Screen-printing technology is employed for the mass production of cost-effective and highly reproducible sensor electrodes, making them suitable for various real-life applications, as mentioned earlier. Consequently, electrochemical sensing techniques have evolved into straightforward, rapid, selective, and low-cost methods. The preparation of SPEs involves multiple steps, including the screen printing of highly conductive inks (metals or active carbon) onto a flat substrate (ceramics or plastics).[9] SPEs consist of two or three electrodes, namely, the working, counter, and, for a three-electrode system, the reference electrode.[10] Carbon nanostructures, such as graphene and carbon nanotubes, with superior electrical, mechanical, and surface characteristics, have proven to be highly effective materials for SPEs. Their appropriate and functional atomic structures, as well as their interaction with other materials makes them highly effective for the development of SPE systems.[11] Furthermore, their electrochemical behaviour results in low background currents and broad potential windows.[9] To improve functionality (electrochemical behaviour, stability, and sensitivity), the surface of SPEs can be appropriately modified. This may involve the addition of various metals, enzymes, complexing agents, polymers, etc., creating an effective sensor system for detecting bioactive components, drug dosages, gene therapy, biological imaging, antibacterial applications, tissue engineering, *etc.*[12,13] Graphene is structured as a two-dimensional (2D) sheet of sp^2 hybridised carbon atoms arranged in a hexagonal (honeycomb) atomic configuration. This stable structure under ambient conditions makes graphene suitable for various sensor applications, including the detection of metals, pharmaceuticals and drugs, glucose, hormones, food dyes, agrochemicals, *etc.*[11,14–16]

Diclofenac (DIC) is a nonsteroidal anti-inflammatory pharmaceutical designed to treat painful conditions, such as

* Corresponding author: Perica Paunović, Ph.D.
Email: pericap@tmf.ukim.edu.mk

arthritis, sprains, strains, gout, migraine, dental pain, and post-surgical discomfort. It effectively reduces pain and inflammation.[17] DIC ranks among the most prevalent pharmaceuticals detected in aquatic environments due to its widespread consumption and limited removal by humans or animals, posing an emerging environmental concern.[18] Thus, the need for a sensitive, rapid, and cost-effective DIC detection method has become crucial. *Da Chuna et al.*[19] proposed the use of an alternative low-cost carbon black and ionic liquid matrix to modify the surface of pencil graphite electrodes (PGE) to quantify DIC in raw materials, intermediates and final products, and mentioned this approach as an interesting alternative for DIC assessment in various pharmaceutical samples. *Reiner et al.*[20] studied various commercial SPEs (multiwalled carbon nanotubes, graphene, graphite, and gold) for the quantitative detection of diclofenac. They employed electrochemical methods, such as cyclic voltammetry, electrogenerated chemiluminescence, and amperometry. *De Carvalho et al.*[21] synthesised cerium dioxide nanoparticles and incorporated them onto a commercial graphite-based SPE for diclofenac level determination. Square wave voltammetry, incorporating cerium dioxide nanoparticles, electrode vacuum heat treatment, and the use of background correction, provided a rapid means of diclofenac detection. *Jahani et al.*[22] suggested an easy experimental method for manufacturing a graphene nanoribbon modified screen-printed electrode, with good selectivity, reproducibility, and sensitivity toward diclofenac and morphine. *Beitollahi et al.*[23] investigated a graphene SPE modified with graphene-Co_3O_4 nanoparticles for detecting morphine in the presence of diclofenac. Their study demonstrated that the modified graphene-Co_3O_4 SPE exhibited superior electrocatalytic activity for morphine oxidation compared to the basic graphene SPE. Additionally, the graphene-Co_3O_4 SPE was explored for the voltammetric determination of diclofenac and morphine in pharmaceutical and biological specimens of morphine ampoule, diclofenac tablet, and urine.

In the past decade, numerous papers have documented the sensing properties of polyvinylidene fluoride (PVDF) and its nanocomposites. Namely, PVDF has been widely studied[24] owing to its exceptional piezoelectric properties, particularly when the polymer is in its electroactive β-phase. These properties have given rise to various applications, especially in the fields of sensing and actuating devices. Even in its stable α-phase, PVDF remains an intriguing material for diverse applications, owing to its superior dielectric constant, chemical inertness, thermal stability, and mechanical properties.

We have previously confirmed and published the sensing activity of carbon nanotube-based SPE electrodes.[25] Subsequently, our experiments were expanded to include other carbon nanostructures, such as graphene and modified graphene, to identify the most suitable carbon sensing nanostructure. In addition to CV and scanning electron microscopy (SEM) analyses, our experiments included UV-Vis methods to examine the oxidation processes. This paper presents the research results stemming from our broader work on the modification of graphene-based SPE nanosensors. A new contribution of this study is the extended application of CV electrochemical procedure for the explicit detection of diclofenac, as well as a detailed characterisation of its electrochemical oxidation through determination of kinetics, the electrochemical mechanism of the process, and the surface characteristics of the investigated SPEs.

2 Experimental

The focus of this study is the commercial graphene SPE (Dropsens Ltd., Llanera, Asturias, Spain), and its modification with polyvinylidene fluoride (PVDF). PVDF was dissolved in *N*,*N*-dimethylacetamide (Merck-Schuchardt) at 2 %wt. concentration, and subsequently applied to the surface of the commercial graphene SPEs. Following application, the PVDF-modified SPE was allowed to dry at ambient temperature.

The sensing activity of both electrodes was investigated concerning commercial DIC. Samples of DicloDuo (Pharma Swiss) were purchased from local pharmacies. The electrolyte used for CV measurements was prepared by diluting DIC in double-distilled water with a conductivity of ≤ 0.1 μS cm^{-1}), mixed with phosphate-buffered solution (PBS). The final concentration of DIC in the PBS solvent was 0.1 g l^{-1} with a pH = 7.4. All reagents and solvents were of analytical grade and used without further purification. The electrochemical behaviour of the studied electrodes was examined through cyclic voltammetry (CV). The electrochemical instrumentation line is presented in Fig. 1. The CV measurements were conducted at ambient temperature using the potentiostat/galvanostat SPELEC – "DROPSENS", (Spain), controlled by the Dropview software package. The conditions for CV measurement were optimised as follows: ambient temperature, 5 scans, potential range from –0.6 to +0.6 V, and automatic current. The cyclic voltammograms were recorded at various scan rates (20, 50, 100, 200, 300, and 400 mV s^{-1}) to determine kinetics of the oxidation process, Tafel plots, and double-layer capacitance of the studied electrodes. The studied SPE electrodes were immersed in the previously mentioned electrolyte with a pH = 7.4. The electrochemical data obtained were processed with Origin 2018 software.

Fig. 1 – Instrumentation line for electrochemical characterisation of the studied electrodes

Physical characterisation of both commercial and modified SPEs was conducted through SEM and UV-Vis spectroscopy. The surface morphology of the SPEs was analysed using

an FEI Quanta 2000 SEM with a secondary electron detector and acceleration voltage of 30 kV under high vacuum. UV-Vis measurements were performed on an Agilent Cary 50/60 UV-Vis spectrophotometer, recording a full identification scan in the wavelength range of 800–200 nm.

3 Results and discussion

3.1 Cyclic voltammetry analysis

To determine the sensitivity of both the commercial SPE graphene electrode and the graphene electrode modified with polyvinylidene fluoride (PVDF) to DIC, electrochemical measurements were performed in a water/PBS solution with a pH = 7.4. This pH value was chosen for its similarity to that in the human body and its ability to produce well-shaped cyclic voltammograms with a satisfactory current response. CV facilitates the determination of characteristic redox reactions occurring on the surfaces of SPE electrodes in interaction with the electrolyte (0.1 mg ml^{-1} in PBS solution, with pH = 7.4). Additionally, CV scanning at different rates v (V s^{-1}) enables the determination of other electrochemical characteristics related to the electrochemical oxidation/reduction of DIC. These include: (i) the rate-determining step (adsorption or diffusion), (ii) the electrochemical mechanism (Tafel slope b, charge transfer coefficient α, and the number of transferred electrons), and (iii) double-layer capacitance C_dl and the ratio of real *vs.* geometric surface area.

Fig. 2 presents the cyclic voltammograms of the studied SPE systems, covering the potential range from –0.6 to +0.6 V with a scanning rate of 50 mV s^{-1}. Both systems exhibited well-shaped peaks characteristic of DIC redox reactions, particularly the G/PVDF SPE system, while the graphene SPE system demonstrated a higher current response (Fig. 2a). This can be attributed to the excellent electrical properties of graphene, facilitated by the bonds between the C atoms within its plane and its conductive bands, making it an excellent conductor of current. The addition of PVDF reduced the electrical conductivity and, consequently, the current response, but not significantly. Three anodic peaks (P_{a1}, P_{a2} and P_{a3}) and one cathodic peak (P_{c2}) were detected (Figs. 2b and 2c), aligning with literature data.[19–21] The electrochemical oxidation and meaning of the oxidation peaks are presented in Fig. 3. The first anodic peak, P_{a1}, corresponds to the upper reaction in Fig. 3, involving a one-electron exchange reaction and the formation of 2,6-dichloroaniline and 2-(2-hydroxyphenyl) acetic acid.[19,26] The second oxidation peak, P_{a2},corresponds to the bottom reaction in Fig. 3, involving the oxidation of 1-hydroxy-2-(hydroxyphenyl) ethanalate (previously formed) to 2-(2-hydroxyphenyl) acetic acid.[25] The opposite reaction is denoted by cathodic peak P_{c2}. The oxidation peaks of DIC are positioned at lower potentials on the graphene SPE electrode, while on the G/PVDF electrode, the potentials are shifted to higher values (Figs. 2b and c). The peak potential separation of the redox pair P_{a2}/P_{c2} for the G|PVDF system was $\Delta E \approx 76$ mV, close to the Nernstian value of 59 mV, suggesting reversibility of the process.[20] For the graphene SPE system, this difference was

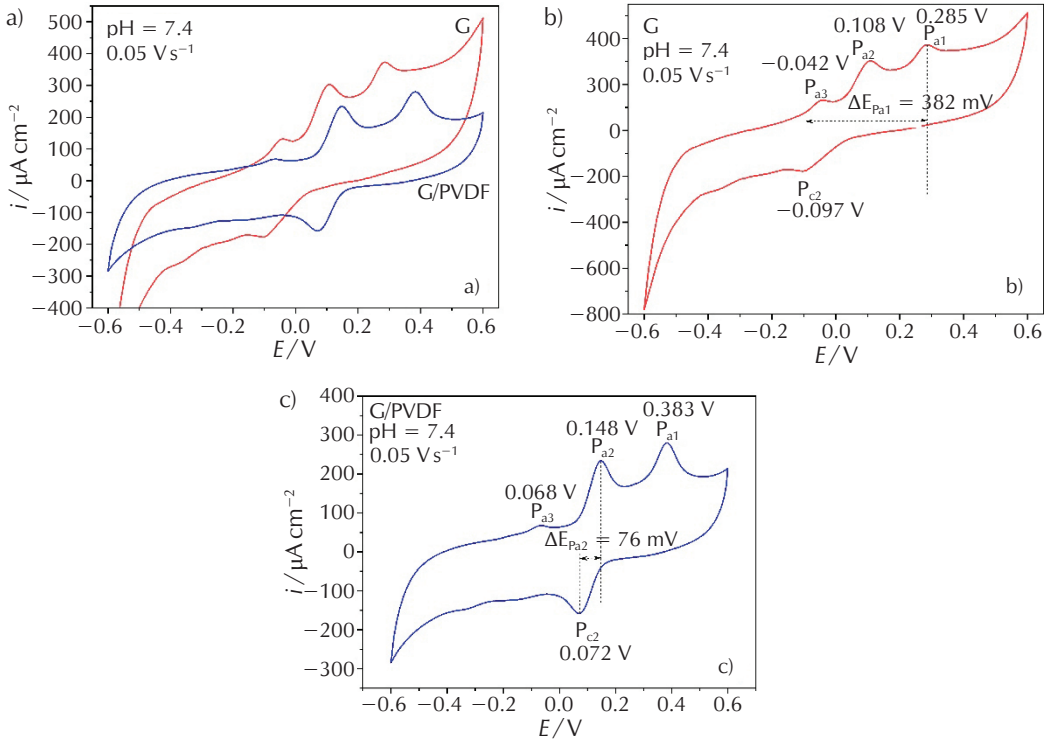

Fig. 2 – Cyclic voltammograms of the studied systems: a) common diagram of both studied systems, b) graphene SPE, and c) G/PVDF-modified SPE, at pH = 7.4 and scan rate of 0.05 V s^{-1}

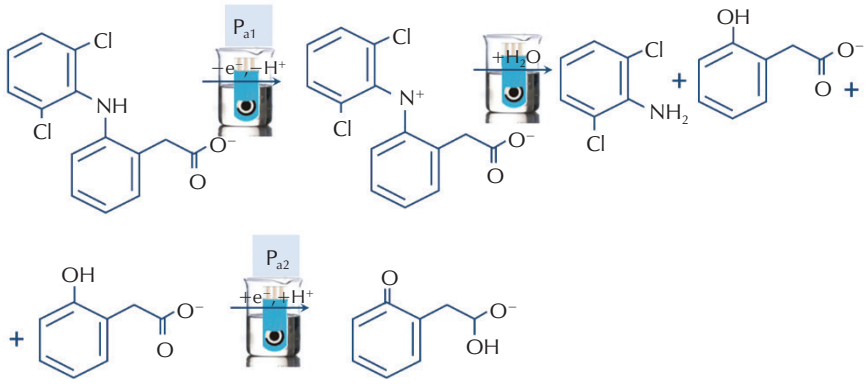

Fig. 3 – Scheme of the electrochemical oxidation of DIC

much higher: $\Delta E \approx 205$ mV, and this process is far from being reversible. The anodic peak P_{a3} is less intense and not well-shaped compared to the previous ones for both studied systems. It corresponds to para-quinonic groups electro-generated at the graphite surface.[19,27], and is positioned at a more negative potential (−0.042 V) for the graphene SPE system compared to that for the G/PVDF system (0.068 V).

3.2 Kinetics and mechanism of the electrochemical oxidation of DIC

As mentioned earlier, cyclic voltammograms scanned at different rates can be employed for the kinetic analysis of the DIC oxidation process. Such voltammograms for both studied systems are presented in Fig. 4. The change in the current response of the first oxidation peak P_{a1} (i_{pa1}) with the change in the scan rate serves as a criterion for determining the limiting step of the electrochemical oxidation of DIC. The most appropriate criterion is the dependence of the logarithm of peak currents on the logarithm of scan rates ($\log i_{Pa1}$–$\log v$).[21,28] The slope of this plot serves as an indicator for the mechanism of the electrochemical oxidation of DIC. A slope value of 1 corresponds to an adsorption-controlled reaction, while a slope value of 0.5 corresponds to the slow diffusion of the reaction species on the electrode surface.[21,27] These plots for both studied SPE systems are presented in Fig. 5.

Both plots demonstrate a very high correlation (> 0.99) for both studied systems. The slope value for graphene SPE electrode was 0.56 (Fig. 5a), close to the value of 0.5, suggesting a diffusion-controlled electrochemical oxidation of DIC.[29,30] The slope for G/PVDF SPE system was 0.78 (Fig. 5b), indicating adsorption as the rate-determining step of the process.[31] The application of a PVDF layer over the graphene surface altered the surface characteristics of the graphene SPE, , consequently changing the mechanism of the electrochemical oxidation of DIC from a diffusion-controlled to an adsorption-controlled process.

The straight-line dependence between the oxidation peak potential E_{Pa1} and logarithm of the scan rate ($\log v$) can be utilised to determine the electrochemical characteristics of the process, such as Tafel slope b and the number of exchanged electrons.

Tafel slope can be calculated using Eqs. (1) or (2):[23,32]

$$E_{Pa_1} = \frac{b}{2} \cdot \log v + \text{const.} \quad (1)$$

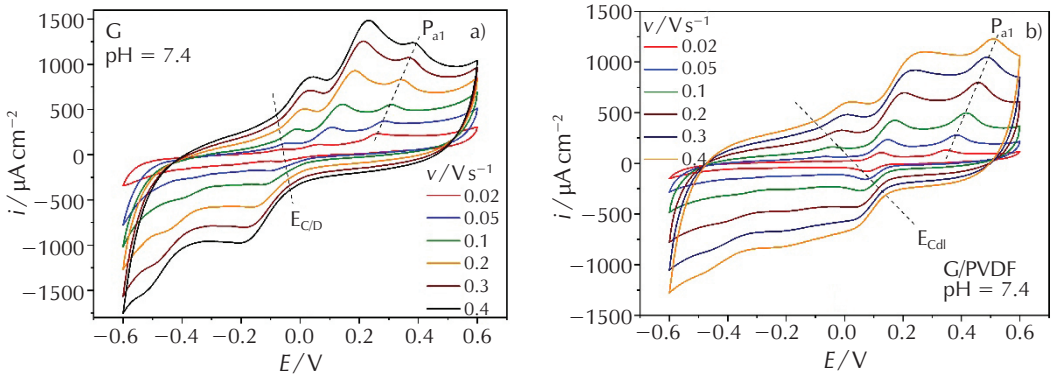

Fig. 4 – Cyclic voltammograms obtained at pH = 7.4 and different scan rates for: a) commercial graphene SPE and b) G/PVDF-modified SPE

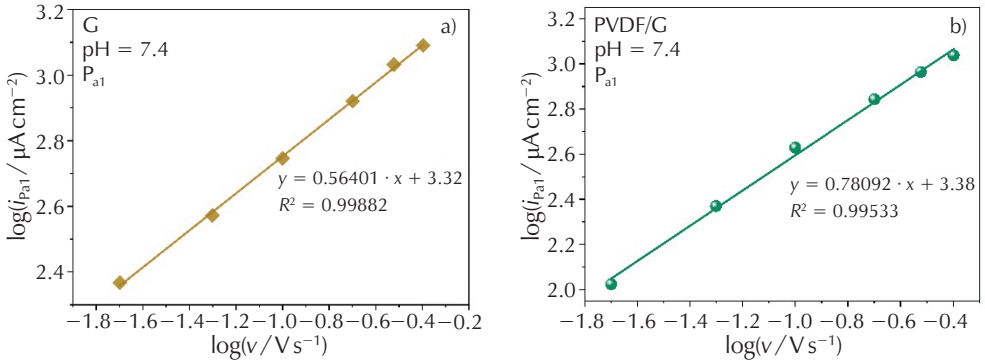

Fig. 5 – Linear fit of log*i* *vs.* log*v* dependence for: a) commercial graphene SPE and b) G/PVDF-modified SPE

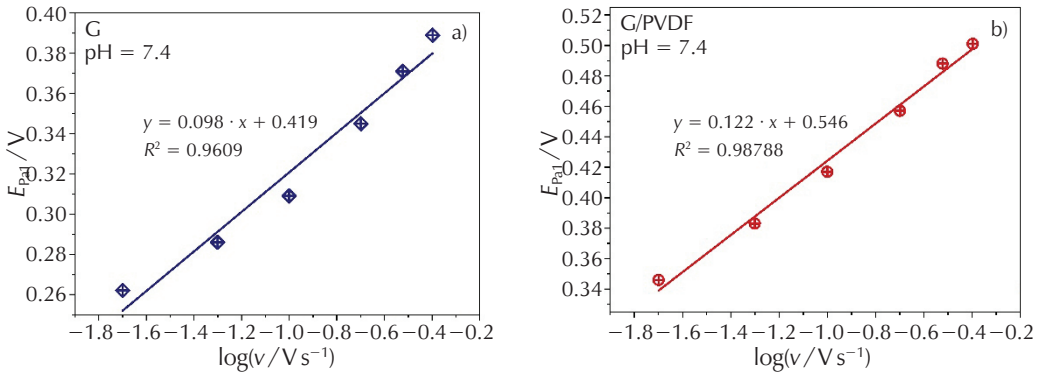

Fig. 6 – Linear fit of E_{Pa1} *vs.* log*v* dependence for a) commercial graphene SPE , and b) G/PVDF-modified SPE

$$\frac{dE_{Pa_1}}{d\log v} = \frac{b}{2} + \text{const.} \quad (2)$$

The E_{Pa1} *vs.* log*v* plots for the studied SPE systems are given in Fig. 6. As evident from the straight-line equations within the diagrams, the Tafel plots are 196 mV dec^{-1} for graphene electrode, and 244 mV dec^{-1} for PVDF electrode.

The charge transferred, *q*, can be calculated using Eq. (3):[33]

$$q = \frac{2.303 \cdot k_B \cdot T}{b \cdot \alpha} \quad (3)$$

where k_B is Boltzman constant ($1.38 \cdot 10^{-23}$ J K^{-1}), *T* is temperature of 298 K, and α is the electron transfer coefficient, which can be calculated using Eq. (4)[33].

$$\alpha = \frac{2.303 \cdot R \cdot T}{b \cdot F} \quad (4)$$

In Eq. (4), *R* is the universal gas constant (8.134 J K^{-1} mol^{-1}), and *F* is the Faraday constant (96485 C mol^{-1}). The charge transferred on both electrodes was $\approx 1.6 \cdot 10^{19}$ C, corresponding to the charge of one electron. This indicates that the number of transferred electrons, *n*, was 1. The calculated values of the parameters from the above equations are presented in Table 1. They suggest that a one-electron transfer process is the rate-determining step of the electrochemical oxidation of DIC.[34,35]

Table 1 – Electrochemical parameters calculated from Eqs. (2)–(4)

SPE electrode	*b* / mV dec^{-1}	α	*n*
G	196	0.3	1
G/PVDF	244	0.24	1

3.3 Surface characteristics of electrodes

The real surface area $A_{r.s.}$ (cm^2) of the electrodes can be determined using the Randles-Sevčik equation (Eqs. (5) or (6)).[36,37]

$$I_{Pa_1} = 2.69 \cdot 10^5 \cdot n^{3/2} \cdot A_{r.s.} \cdot C \cdot D_{DIC}^{1/2} \cdot v^{1/2} \quad (5)$$

$$A_{r.s.} = \frac{\frac{dI_{Pa_1}}{dv^{1/2}}}{2.69 \cdot 10^5 \cdot n^{3/2} \cdot C \cdot D_{DIC}^{1/2}} \quad (5)$$

I_{Pa1} is a current (μA) of the P_{a1} oxidation peak in the cyclic voltammograms (Fig. 4), *v* is scan rate (V s^{-1}), *n* is the number

of exchanged electrons in the electrochemical oxidation of DIC, C is the concentration (mol cm^{-3}) of active molecule, *i.e.*, diclofenac, and D is the diffusion coefficient (cm^2 s^{-1}) of the oxidised reduced species of DIC. The number of exchanged electrons n, was 1. The concentration of diclofenac in the solution was 0.1 g l^{-1} or 3.38 · 10^{-7} mol cm^{-3}. The diffusion coefficient D was 1.072 · 10^{-8} cm^2 s^{-1}.[38] The slope of the linear plot between the anodic current peaks I_{Pa1} (μA) and the square root of the scan rate v (V s^{-1}) is the value of the numerator in Eq. (6). These values for both studied systems can be seen in the straight-line equations in Fig. 7. The real surface areas were determined to be 29.95 cm^2 for the graphene electrode, and 27.24 cm^2 for the G/PVDF electrode. The application of a PVDF layer over the graphene surface also reduced the real surface area of the graphene electrode, consequently leading to a lower current response, as observed in the cyclic voltammograms presented in Fig. 2.

The ratio of the real surface area of the graphene and G/PVDF electrodes can also be estimated through the values of double-layer capacitance (C_{dl}). The voltammograms shown in Fig. 4 can be utilised to determine C_{dl}. At the intersection of the voltammograms (E_{Cdl} line) in the region of charge and discharge of the electrochemical double layer, the double-layer capacity (C_{dl}) of the studied electrodes can be determined from the corresponding values of anodic and cathodic currents densities, using Eq. (7).[39]

$$C_{dl} = \frac{\mathrm{d}i_{cap.}}{\mathrm{d}\left(\frac{\partial E}{\partial t}\right)} = \frac{\mathrm{d}i_{cap.}}{\mathrm{d}v} \tag{7}$$

The capacitance current density $i_{cap.}$ at a given scanning rate was calculated as the mean value of the absolute values of the anode and cathode currents at the potentials on the intersection E_{Cdl}. The plot $i_{cap.}$ *vs.* v is a straight-line and its slope is the value of the double-layer capacity, C_{dl}. These plots for the studied SPE systems are presented in Fig. 8. As evident, the calculated value for the double-layer capacity of the graphene electrode was 0.94 mF cm^{-2}, while the corresponding value for the G/PVDF electrode was 0.8 mF cm^{-2}. The ratio of these values is equal to the ratio of the real surface area of both electrodes, which in this case was 1.17. This value is in good agreement with the value of 1.1 – the surface area ratio determined using Randles-Sevčik equation for the determination of the real surface area. The relative error was ≈6 %.

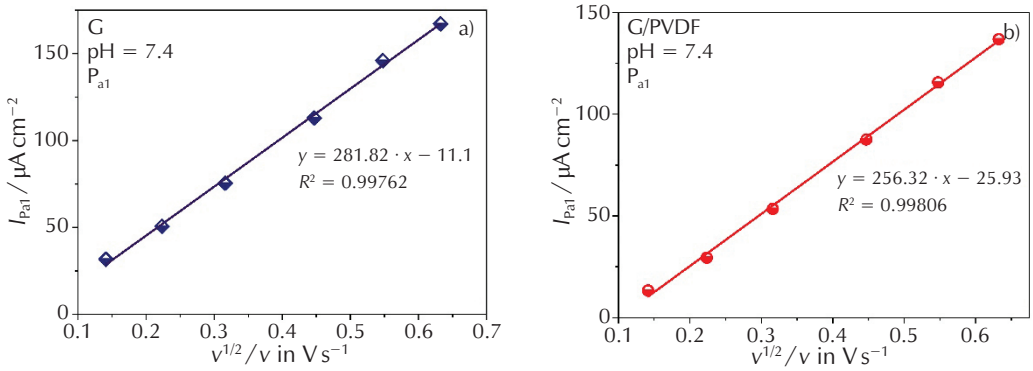

Fig. 7 – Linear fit of I *vs.* $v^{1/2}$ dependence for:
a) commercial graphene SPE and b) G/PVDF-modified SPE

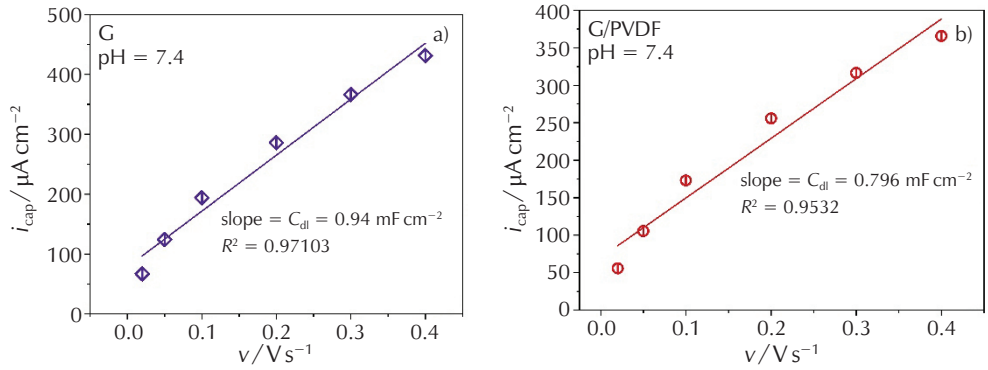

Fig. 8 – Linear fit of log$i_{cap.}$ *vs.* log$v$ dependence for:
a) commercial graphene SPE and b) G/PVDF-modified SPE

3.4 Physical characterisation

The morphology of the studied electrode systems was observed by SEM, and the SEM images are presented in Fig. 9. In Fig. 9a, the surface of the graphene electrode at lower magnification is displayed, revealing a smooth surface. At higher magnification (Fig. 9b), layers of graphene with an irregular structure are evident, resulting in a rough surface that explains the good current response. The formation of a polymer layer is visible in Fig. 9c for the PVDF-modified graphene electrode (G/PVDF). Different surface morphology can be observed compared to the commercial graphene electrode, where the PVDF polymer film did not cover the entire surface of the SPE electrode, leading to a decrease in surface roughness. However, with the application of the polymer drop on the graphene surface, the increased functionality on the graphene was expected, explaining the better-shaped cyclic voltammograms. At higher magnification (Fig. 9d), the fibrillar structure of the polymer film can be observed.

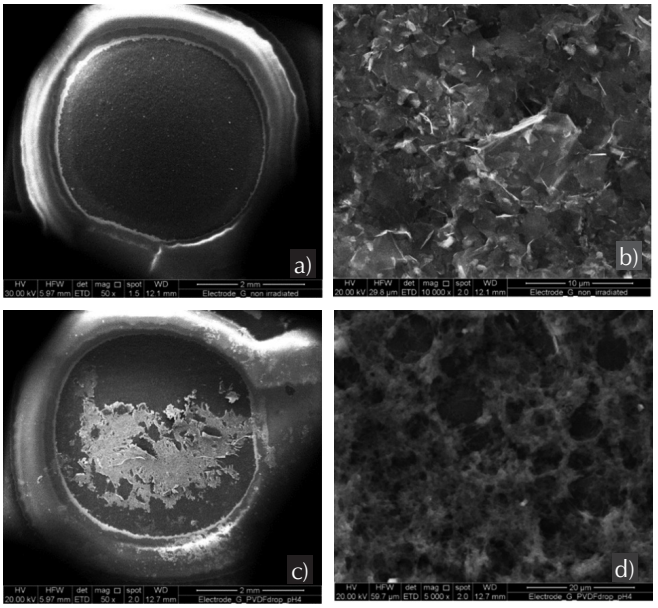

Fig. 9 – SEM images of surface morphology of: a) commercial graphene SPE , magnification ×50, b) commercial graphene SPE, magnification ×5000, c) G/PVDF-modified SPE, magnification ×50, and d) G/PVDF-modified SPE, magnification ×5000

The fresh electrolyte before and after CV measurements (DIC 0.1 g l^{-1} in PBS, pH = 7.4) was studied using UV-Vis spectroscopy. Fig. 10 presents the corresponding UV-Vis spectra. The wavelengths at which the characteristic UV-Vis peaks appear and their corresponding absorbance values are given in Table 2. UV-Vis analysis indicates that the solution underwent current-induced changes during the CV measurements. This effect was minor, as indicated by a shift of the UV-Vis peak of DIC (usually ≈ 300 nm) from 276.1 to 275.4 nm, while the peak absorbance value decreased from 0.316 to 0.257. This decrease is attributed to the oxidation of DIC in the solvent due to the flow of electricity.[40] The general conclusion from the UV-Vis analysis is that the current during the CV measurement induced structural changes in the solutions, as reflected in the change in absorbance. The detected effect was weak but still noticeable. The reason for this weak effect could be attributed to the neutral solution environment (pH = 7.4).

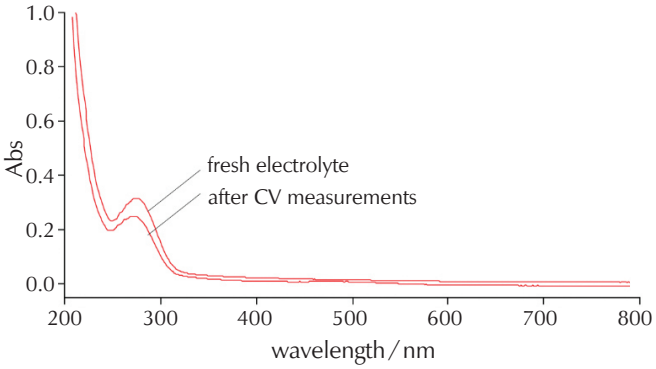

Fig. 10 – UV-Vis spectra of the electrolyte (0.1 g l^{-1} DIC in PBS, pH = 4) before and after electrochemical measurements

Table 2 – Wavelength and absorbance values of UV-Vis peaks in solution of DIC in PBS (0.1 g l^{-1}, pH = 7.4)

	Wavelength / nm	Absorbance
Fresh electrolyte	276.1	0.316
After CV measurements	275.4	0.257

4 Conclusion

This research sought to establish a straightforward, rapid, and cost-effective method employing graphene-based screen-printed electrodes (SPEs) for the highly sensitive medical detection of diclofenac (DIC). Both the graphene SPE electrode and its modification with PVDF (G/PVDF) were studied. According to the findings presented, the following conclusions can be drawn: Both systems exhibited well-shaped rectangular cyclic voltammograms with a high current response. The G/PVDF system displayed slightly better-shaped rectangular voltammograms, higher reversibility, but a slightly lower current response compared to the graphene SPE.

The superior current response of the graphene electrode is a result of its better surface area, as evidenced by both the ratio of the real surface area determined by the Randles-Sevčik equation and the ratio of the C_{dl} values. The better shaping of the G/PVDF voltammograms is attributed to the increased functionality on the graphene surface resulting from PVDF application. SEM analysis revealed that the higher surface area of the graphene electrode is a result of the irregular structure of the graphene, while PVDF application reduced surface roughness.

During the voltammetric measurements, in the used electrolyte containing the sensed substance (DIC), weak but still noticeable structural changes were detected by UV-Vis analysis.

The studied SPE systems demonstrated appropriate selectivity, current response, and reproducibility, positioning themselves as suitable electrodes for the sensitive, rapid, and cost-effective detection of DIC.

ACKNOWLEDGEMENTS

This paper was realised within the bilateral scientific project between Faculty of Technology and Metallurgy, Ss. Cyril and Methodius University in Skopje, and Montanuniversität Leoben – Department Kunststofftechnik, Austria, supported by the Ministry of Education and Science of Republic of North Macedonia.

List of abbreviations and symbols

$A_{r.s.}$ – real surface area
b – Tafel plot
C_{dl} – double-layer capacity
D_{DIC} – diffusion coefficient of diclofenac
E – potential
F – Faraday constant
I – current
i – current density
$i_{cap.}$ – capacitance current density
k_B – Boltzman constant
n – number of exchanged electrons
q – electrical charge
T – temperature
t – time
v – scanning rate
α – electron transfer coefficient
CV – cyclic voltammetry
DIC – diclofenac
G – graphene
PBS – phosphate-buffered solution
PVDF – polyvinylidene fluoride
SEM – scanning electron microscopy
SPE – screen-printed electrodes
UV-Vis – ultraviolet-visible

References
Literatura

1. *S. A. Ozkan, J.-M. Kauffmann, P. Zuman*, Electroanalysis in biomedical and pharmaceutical sciences, Monographs in electrochemistry, Springer-Verlag, Berlin Heidelberg, 2015, p. 119–140, doi: https://doi.org/10.1007/978-3-662-47138-8_5.
2. *P. N. Badyal, C. Sharma, N. Kaur, R. Shankar, A. Pandey, R. K. Rawal*, Analytical Techniques in Simultaneous Estimation: An Overview, Austin J. Anal. Pharm. Chem. **2** (2015) 1037.
3. *E. de Rycke, C. Stove, P. Dubrel, S. de Saeger, N. Beloglazova*, Recent developments in electrochemical detection of illicit drugs in diverse matrices, Biosens. Bioelectron. **169** (2020) 112579, doi: https://doi.org/10.1016/j.bios.2020.112579.
4. *A. Hayat, J. L. Marty*, Disposable screen printed electrochemical sensors: tools for environmental monitoring, Sensors **14** (2014) 10432–10453, doi: https://doi.org/10.3390/s140610432.
5. *M. R. Siddiqui, Z. A. AlOthman, N. Rahman*, Analytical techniques in pharmaceutical analysis: A review, Arabian J. Chem. **10** (2017) S1409–S1421, doi: https://doi.org/10.1016/j.arabjc.2013.04.016.
6. *M. A. Balbino, E. N. Oiye, M. F. M. Ribeiro, J. W. Cruz Júnior, I. C. Eleotério, A. J. Ipólito, M. F. de Oliveira*, Use of screen-printed electrodes for quantification of cocaine and Δ^9-THC: adaptions to portable systems for forensic purposes, J. Solid State Electrochem. **20** (2016) 2435–2443, doi: https://doi.org/10.1007/s10008-016-3145-3.
7. *M. Li, Y.T. Li, D.W. Li, Y.T. Long*, Recent developments and applications of screen-printed electrodes in environmental assays – A review, Anal. Chim. Acta **734** (2012) 31–44, doi: https://doi.org/10.1016/j.aca.2012.05.018.
8. *F. Arduini, L. Micheli, D. Moscone, G. Palleschi, S. Piermarini, F. Ricci, J. Volpe*, Electrochemical biosensors based on nanomodified screen-printed electrodes: Recent applications in clinical analysis, Trends Anal. Chem. **79** (2016) 114–126, doi: https://doi.org/10.1016/j.trac.2016.01.032.
9. *J. Wang, B. Tian, V. B. Nascimento, L. Angnes*, Performance of screen-printed carbon electrodes fabricated from different carbon inks, Electrochim. Acta **43** (1998) 3459–3465, doi: https://doi.org/10.1016/S0013-4686(98)00092-9.
10. *P. Lakhera, V. Chaudhary, A. Jha, R. Singh, P. Kush, P. Kumar*, Recent developments and fabrication of the different electrochemical biosensors based on modified screen printed and glassy carbon electrodes for the early diagnosis of diverse breast cancer biomarkers, Mater. Today Chem. **26** (2022) 101129, doi: https://doi.org/10.1016/j.mtchem.2022.101129.
11. *R. M. Silva, L. M. Meireles, A. D. Da Silva, J. R. Camargo, B. S. de Castro, P. S. Silva, B. C. Janegitz, T. A. Silva,* Carbon nanomaterials-based screen-printed electrodes for sensing applications, Biosensors **13** (2023) 453, doi: https://doi.org/10.3390/bios13040453.
12. *H. Shen, L. Zhang, M. Liu, Z. Zhang*, Biomedical applications of graphene, Theranostics **2** (2012) 283–294, doi: https://doi.org/10.7150/thno.3642.
13. *L. Feng, Z. Liu*, Graphene in biomedicine: opportunities and challenges, Nanomedicine **6** (2011) 317–324, doi: https://doi.org/10.2217/nnm.10.158.
14. *D. Thirumalai, S. Lee, M. Kwon, H.-J. Paik, J. Lee, S.-C. Chang*, Disposable voltammetric sensor modified with block copolymer-dispersed graphene for simultaneous determination of dopamine and ascorbic acid in *ex vivo* mouse brain tissue, Biosensors **11** (2021) 368, doi: https://doi.org/10.3390/bios11100368.

15. *H. Karimi-Maleh, H. Beitollahi, P. S. Kumar, S. Tajik, P. Jahani, F. Karimi, C. Karaman, Y. Vasseghian, M. Baghayeri, J. Rouhi, P. Show, S. Rajendran, F. Li, N. Zare*, Recent advances in carbon nanomaterials-based electrochemical sensors for food azo dyes detection, Food Chem. Toxicol. **164** (2022) 112961, doi: https://doi.org/10.1016/j.fct.2022.112961.
16. *Garima, A. Sachdev, I. Matai*, An electrochemical sensor based on cobalt oxyhydroxide nanoflakes/reduced graphene oxide nanocomposite for detection of illicit drug-clonazepam, J. Electroanal. Chem. **919** (2022) 116537, doi: https://doi.org/10.1016/j.jelechem.2022.116537.
17. URL: https://patient.info/medicine/diclofenac-for-pain-and-inflammation-diclodent-dicloflex-diclomax-diclo-sr-econac-enstar-xl-motifene-voltarol.
18. *Z. Xie, Y. Gan, J. Tang, S. Fan, X. Wu, X. Li, H. Cheng, J Tang*, Combined effects of environmentally relevant concentrations of diclofenac and cadmium on *Chironomus riparius larvae*, Ecotoxicol. Environ. Saf. **202** (2022) 110906, doi: https://doi.org/10.1016/j.ecoenv.2020.110906.
19. *C. E. P. da Cunha, E. S. B. Rodrigues, M. F. Alecrim, D. V. Thomaz, I. Y. L. Macêdo, L. F. Garcia, J. R. de Oliveira Neto, E. K. G. Moreno, N. Ballaminut, E. de Souza Gil*, Voltammetric evaluation of diclofenac tablets samples through carbon black-based electrodes, Pharmaceuticals **12** (2019) 83, doi: https://doi.org/10.3390/ph12020083.
20. *C. Reiner, A. Habekost*, (Spectro-) Electrochemical detection of diclofenac with different screen-printed electrodes, Int. J. Sci. Eng. Invest. **6** (2017) 54–62.
21. *R. C. de Carvalho, A. J. Betts, J. F. Cassidy*, Diclofenac determination using CeO_2 nanoparticle modified screen-printed electrodes – A study of background correction, Microchem. J. **158** (2020) 105258, doi: https://doi.org/10.1016/j.microc.2020.105258.
22. *P. M. Jahani, S. Z. Mohammadi, A. Khodabakhshzadeh, J. H. Cha, M. S. Asl, M. Shokouhimehr, K. Zhang, Q. V. Le, W. Peng*, Simultaneous detection of morphine and diclofenac using graphene nanoribbon modified screen-printed electrode, Int. J. Electrochem. Sci. **15** (2020) 9037–9048, doi: https://doi.org/10.20964/2020.09.14.
23. *H. Beitollahi, M. Hamzavi, M. Torkzadeh-Mahani*, Electrochemical determination of hydrochlorothiazide and folic acid in real samples using a modified graphene oxide sheet paste electrode, Mater. Sci. Eng. C **52** (2015) 297–305, doi: https://doi.org/10.1016/j.msec.2015.03.031.
24. *A. Ferrreira, J. G. Rocha, A. Ansón-Casaos, M. T. Martínez, F. Vaz, S. Lanceros-Mendez*, Electromechanical performance of poly(vinylidene fluoride)/carbon nanotube composites for strain sensor applications, Sens. Actuators, A **178** (2012) 10–16, doi: https://doi.org/10.1016/j.sna.2012.01.041.
25. *A. Grozdanov, P. Paunović, I. Dimitrievska, M. Barsbay, Z. Arsova Sarafinovska,* Electrochemical detection and evaluation of diclofenac chloride with modified screen-printed electrodes, Mater. Sci. Eng. Int. J. **7** (2023) 158–164, doi: https://doi.org/10.15406/mseij.2023.07.00219.
26. *G. Y. Aguilar-Lira, G. A. Álvarez-Romero, A. Zamora-Suárez, M. Palomar-Pardavé, A. Rojas-Hernández, J. A. Rodríguez-Ávila, M. E. Páez-Hernández*, New insights on diclofenac electrochemistry using graphite as working electrode, J. Electroanal. Chem. **794** (2017) 182–188, doi: https://doi.org/10.1016/j.jelechem.2017.03.050.
27. *E. S. Gil, R. O. Couto*, Flavonoid electrochemistry: a review on the electroanalytical applications, J. Pharmacogn. **23** (2013) 542–558, doi: https://doi.org/10.1590/S0102-695X2013005000031.
28. *U. Ciltas, B. Yilmaz, S. Kaban, B. K. Akcay, G. Nazik*, Study on the interaction between isatin-β-thiosemicarbazone and calf thymus DNA by spectroscopic techniques. Iran. J. Pharm. Res. **15** (2014) 715–722, doi: https://doi.org/10.22037/ijpr.2015.1691.
29. *S. Guan, X. Fu, B. Zhang, M. Lei, Z. Peng*, Cation-exchange-assisted formation of NiS/SnS_2 porous nanowalls with ultrahigh energy density for battery–supercapacitor hybrid devices, J. Mater. Chem. A **6** (2020) 3300–3310, doi: https://doi.org/10.1039/C9TA11517J.
30. *G. A. J. Merghani, A. A. Elbashir*, Development of chemically modified electrode using cucurbit(6)uril to detect ranitidine hydrochloride in pharmaceutical formulation by voltammetry, J. Anal. Pharm. Res. 7 (2018) 634–639. doi: https://doi.org/10.15406/japlr.2018.07.00294.
31. *G. A. Jothi Grace, A. Gomathi, C. Vedhi*, Electrochemical behaviour of 1,4-diaminoanthra-9,10-quinone at conducting polymer based modified electrode, J. Nanosci. Technol. **2** (2016) 209–212.
32. *W. He, Y. Ding, W. Zhang, L. Ji, X. Zhang, F. Yang*, A highly sensitive sensor for simultaneous determination of ascorbic acid, dopamine and uric acid based on ultra-small Ni nanoparticles, J. Electroanal. Chem. **775** (2016) 205–211, doi: https://doi.org/10.1016/j.jelechem.2016.06.001.
33. *E. Gileadi*, Electrode Kinetics for Chemists, Chemical Engineers, and Materials Scientists, VCH Publishers Inc., New York, 1993.
34. *M. Shamsipur, M. Najafi, M.-R. Milani-Hosseini*, Highly improved electrooxidation of glucose at a nickel(II) oxide/multi-walled carbon nanotube modified glassy carbon electrode, Bioelectrochemistry **77** (2010) 120–124, doi: https://doi.org/10.1016/j.bioelechem.2009.07.007.
35. *R. Guidelli, R. G. Compton, J. M. Feliu, E. Gileadi, J. Lipkowski, W. Schmickler, S. Trasatti*, Definition of the transfer coefficient in electrochemistry (IUPAC Recommendations 2014), Pure Appl. Chem. **86** (2014) 245–258, doi: https://doi.org/10.1515/pac-2014-5025.
36. *P. Zanello*, Inorganic Electrochemistry, Theory, Practice and Application, Royal Society of Chemistry, Cambridge, 2003.
37. *A. Grimaldi, G. Heijo, E. Méndez*, A multiple evaluation approach of commercially available screen-printed nanostructured carbon electrodes, Electroanalysis **26** (2014) 1684–1693, doi: https://doi.org/10.1002/elan.201400122.
38. *Y. Maitani, H. Sato, T. Nagai*, Effect of ethanol on the true diffusion coefficient of diclofenac and its sodium salt in silicone membrane, Int. J. Pharm. **113** (1995) 165–174, doi: https://doi.org/10.1016/0378-5173(94)00192-8.
39. *L. M. da Silva, L. A. de Faria, J. F. C. Boodts*, Determination of the morphology factor of oxide layers, Electrochim. Acta **47** (2001) 395–403, doi: https://doi.org/10.1016/S0013-4686(01)00738-1.
40. *M. K. Hasan, M. A. Hossain, A. Sultana, M. Shoeb, N. Nahar*, Evaluation of Diclofenac by UV-Vis Spectrophotometer in Some Locally Produced Tablets, Dhaka Univ. J. Sci. **65** (2017) 163–165, doi: https://doi.org/10.3329/dujs.v65i2.54525.

SAŽETAK

Voltametrijska detekcija diklofenaka sitotiskanim elektrodama na bazi grafena i PVDF-modificiranog grafena

Perica Paunović, Anita Grozdanov, Iva Dimitrievska* i *Ana Tomova*

Identifikacija i kvantifikacija brojnih lijekova i drugih farmaceutskih proizvoda u različitim medijima postali su ključni aspekti u suvremenoj zdravstvenoj zaštiti i upravljanju okolišem. Elektrokemijske metode, osobito one koje koriste sitotiskane elektrode i različitu prijenosnu opremu, pokazale su se kao brzim, učinkovitim, osjetljivim i ekonomičnim analitičkim pristupom. Fokus ovog istraživanja bio je na detekciji protuupalnog lijeka diklofenaka u neutralnom mediju. S ciljem identifikacije diklofenaka te određivanja kinetike i elektrokemijskog mehanizma njegove oksidacije, primijenjena je metoda cikličke voltametrije. Procijenjene su i površinske karakteristike primijenjenih sitotiskanih elektroda. U tu svrhu ispitana je primjenjivost grafenskih i modificiranih grafenskih sitotiskanih elektroda kao nanosenzora. Površina grafenskih sitotiskanih elektroda modificirana je kapljičnim postupkom primjenom poliviniliden fluorida. Morfologija sitotiskanih elektroda analizirana je skenirajućom elektronskom mikroskopijom, a elektrolit (0,1 g diklofenaka u litri fosfatnog pufera, pH = 7,4) UV-Vis spektroskopijom. Dobiveni rezultati ukazuju na potencijal proučavanih elektroda za detekciju diklofenaka.

Ključne riječi
Sitotiskane elektrode, nanosenzori, ciklička voltametrija, grafen, kapljična modifikacija PVDF, diklofenak

Tehnološko-metalurški fakultet, Univerzitet "Sv. Kiril i Metodij" u Skopju, Rudjer Bošković 16, Skopje 1000, Sjeverna Makedonija

Izvorni znanstveni rad
Prispjelo 22. studenoga 2023.
Prihvaćeno 19. siječnja 2024.